Chapter 2

FORMATION OF THE K-CORONA AND THE FOCUS OF THIS RESERACH

2.1 The K-corona

The K-coronal spectrum, as described in chapter-**1,** is the coronal brightness attributed to the photospheric spectrum scattered off the free electrons in the solar corona. The existence of the free electrons is due to the high temperatures prevalent in the solar corona. This scattering phenomenon is commonly known as Thomson scattering. This brightness is only revealed during a total solar eclipse.

2.2 The photospheric spectrum

Figure (**2.1**) shows the solar spectrum in the visible region, as it would appear above the earth's atmosphere. The shape of the photospheric spectrum is similar in nature, however, with a much greater flux. As evident from the solar spectrum the visible region is replete with absorption lines. Among the deep and conspicuous absorption lines, which were labeled by Fraunhofer, are the calcium H and K lines at 3968.5 angstrom and 3933.7 angstrom, respectively. The dark Fraunhofer lines observed in the

solar spectrum are caused by selective process of line scattering or line absorption, accompanied by continuum absorption.

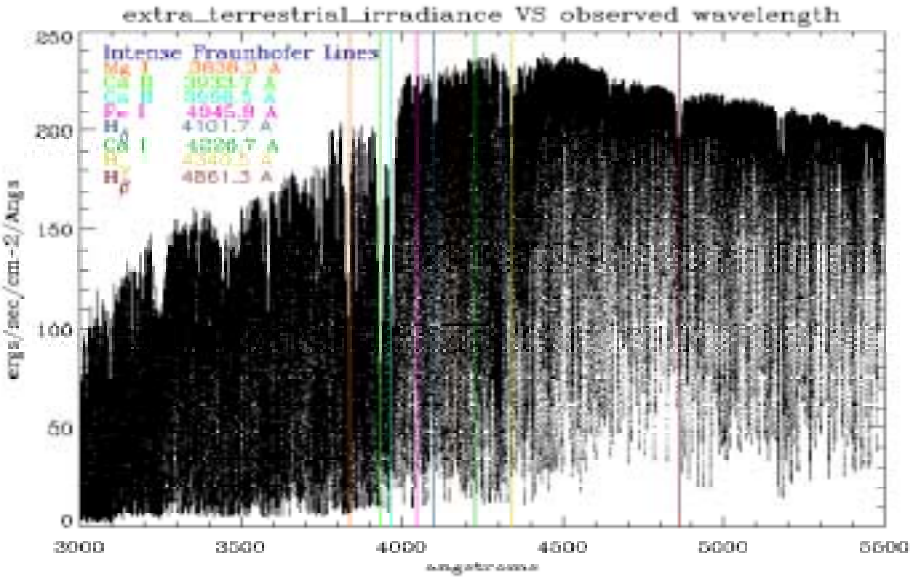

Figure (2.1). This is a plot of the extraterrestrial solar irradiance spectrum. This was obtained by starting with the ground-based Fourier Transform Spectrometer at the McMath/Pierce Solar Telescope at Kitt Peak, Arizona, and then correcting for wavelength-dependent absorption in the Earth's atmosphere

2.3 The scattering source

The scattering source for the formation of the K-corona is the free electrons in the solar corona. For a corona of one million Kelvin these free electrons have a mean thermal velocity of ~ 5500 km/sec and given by equation (**2.1**).

$$\mathbf{v = \sqrt{\frac{2kT}{m}}\ where} \qquad \mathbf{(2.1)}$$

$$\mathbf{k = Boltzmann\ \ constant = 1.38 \times 10^{-23}\ J/K}$$

$$\mathbf{m = Electron\ \ mass = 9.11 \times 10^{-31}\ kg}$$

$$\mathbf{T = Coronal\ \ temperature \sim 10^{6}\ K}$$

In an equilibrium state the electron velocity distribution can be described as Maxwelian in the solar corona where the electron number density in the vicinity of the solar limb is $\sim 10^{8}$ cm^{-3}. This means that due to frequent collisions the velocity distribution is the same in all coordinates. However cataclysmic phenomena such as flares or coronal mass ejection can cause a deviation from a Maxwellian distribution locally. Furthermore, in the case of dilute plasma where collisions are infrequent the velocities may differ in different directions. This may be more pronounced in the interplanetary space where the particles stream from the sun in one direction.

2.4 The effects on the incident radiation by the scattering source

In section (**2.3**) it was shown that a free coronal electrons move with an average thermal velocity of ~5500.0 km/sec in a corona of million degree Kelvin. Such motions are called **Thermal Motions**. This also means that a photon of wavelength (λ) incident in an electron will be Doppler broadened by equation (**2.2**).

$$\Delta\lambda = \lambda \times \frac{v}{c} \quad \text{where} \qquad \textbf{(2.2)}$$

$v \sim 5500$ km/sec for $T = 1.0$ MK

$c = 3 \times 10^5$ km/sec

From equation (**2.2**) for an incident wavelength at 4000.0 angstrom the broadening is ~70.0 angstroms. This phenomenon is called **Thermal Doppler Broadening**. This broadening increases with increasing thermal velocities for the electrons, which in turn depend on the coronal temperature. This phenomenon could be expected to cause all the narrow absorption lines, as evident in figure (**2.1**), to smooth into a continuum upon incidence with the coronal electrons. However weak depressions are still expected in the vicinity of the deep Fraunhofer lines thus smoothening the small-scale depressions while preserving the large-scale depressions. This near-total obliteration of the deep Fraunhofer lines by the thermal Doppler broadening served as one of the first clues for a hot corona. From equation (**2.1**) and equation **(2.2**) it is evident that the extent of smoothening ($\Delta\lambda$) is related to the coronal temperature (**T**) by equation (**2.3**).

$$\Delta\lambda \sim \sqrt{T} \qquad \textbf{(2.3)}$$

Once the radiation is incident on the electrons the scattering process is independent of wavelength and equal numbers of photons are scattered forwards and backwards. That is the scattering is coherent in the rest frame of the electrons. Since the scattering source itself is in thermal motion the radiation reaching the observer is **Doppler shifted**. In addition to the thermal velocity the coronal electrons may also acquire velocity due to turbulence.

2.5 The K-coronal spectrum

The photospheric radiation scattered off the free coronal electrons is known as the K-coronal radiation. Cram (1976) presented a physical model for the formation of the K-corona based on the Thomson scattering of the photospheric radiation by the free electrons in the solar corona. In figure (**2.2**) a schematic drawing of Cram's model is shown. Here a known electron density distribution, determined by other independent means, is assumed for all positions along the line of sight. The normal to the line of sight from the center of the sun is at a distance (ρ).

Each point on the line of sight has certain number of electrons and is subject to collisions with photons that make up the photospheric spectrum. The electrons at a particular point on the line of sight are exposed to the same photospheric spectrum from all the points on the solar surface that they see and are subjected to Thomson scattering. However the photospheric radiation incident on these electrons are also subjected to the **limb-darkening effect.** That is the brightness of the incident radiation is decreased as the

radiation from the edges travel through thicker and thicker levels on the solar atmosphere to reach the electrons. The limb darkening is wavelength dependent. The limb-darkening effect is most noticeable in the visible wavelength region.

The thermal Doppler broadened scattered radiation observed by an observer on earth, due to Thomson scattering, is the accumulation of all the radiation that is scattered in the direction of the line of sight of the observer by all the electrons lying along the line of sight.

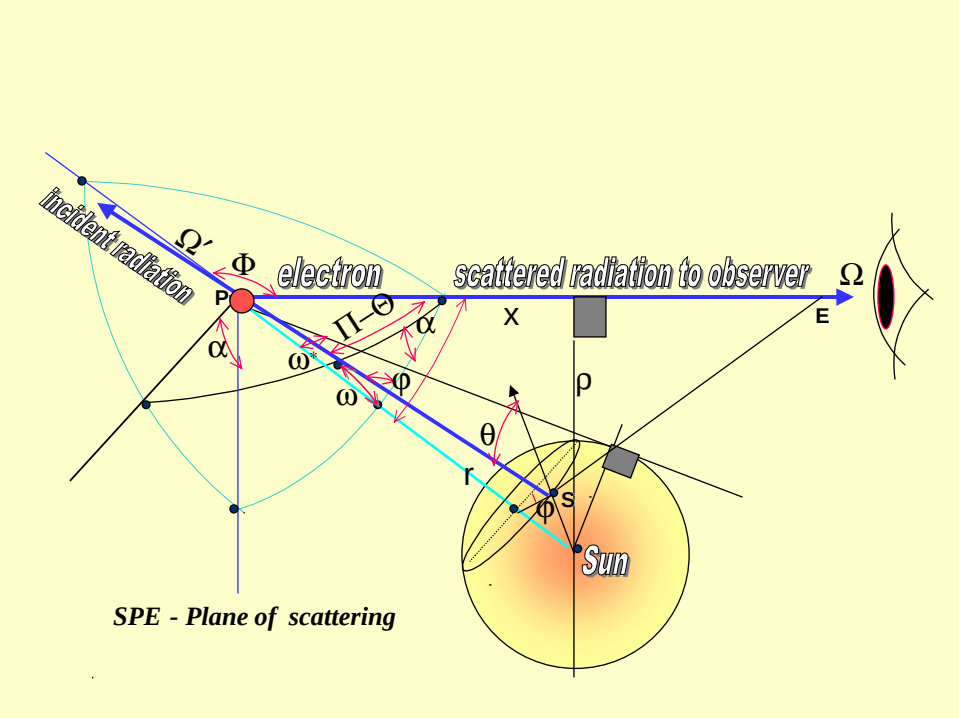

Figure (2.2). The photospheric radiation is emitted from a point S on the surface of the sun. The electrons at point P in the corona scatter some of the incident radiation towards a terrestrial observer at E, which is known as K-coronal radiation.

Figure (**2.3**) shows a modeled spectrum for the scattered wavelength for an independently measured electron number density, given by equation (**5.7**), along the line of sight at 1.1 solar radii from the center of the sun. Here an isothermal corona was assumed and the plot shows models for different isothermal coronal temperatures.

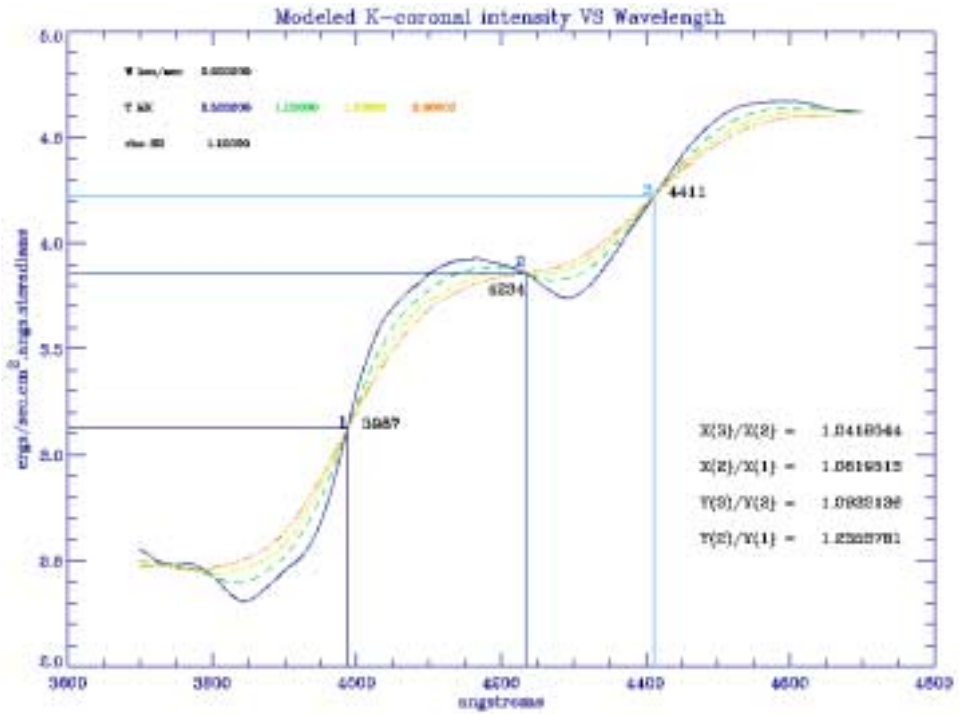

Figure (2.3). This plot shows the modeled K-coronal intensity spectra against wavelength. The composite plots are for different isothermal temperatures assumed for the solar corona for a given line of sight at 1.1 solar radii.

As predicted in section (**2.3**) the modeled K-coronal intensity spectrum, as depicted in figure (**2.3**) for a line of sight at 1.1 solar radii, is very much smoother than the shape of the radiation incident on the coronal electrons. From the shape of the incident radiation spectrum, as is shown in figure (**2.1**), the vertical spread in the intensity

reflects the existence of millions of narrow absorption lines together with wide absorption lines. These millions of narrow lines in the incident radiation have been completely washed away, as revealed in figure (**2.3**), giving rise to a continuous spectrum. However the large-scale depressions are preserved.

Figure (**2.4**) and figure (**2.5**) show the modeled K-coronal intensity spectra for lines of sight at 1.3 and 1.5 solar radii, respectively.

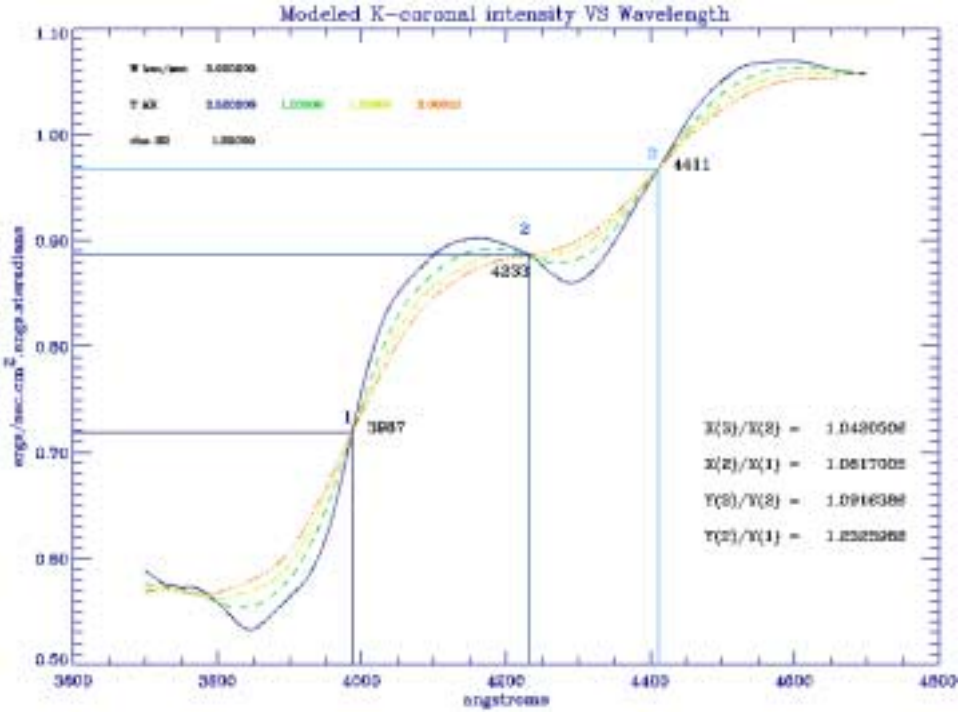

Figure (2.4). Modeled K-coronal intensity spectrum against wavelength for different isothermal coronal temperatures for a given line of sight at 1.3 solar radii.

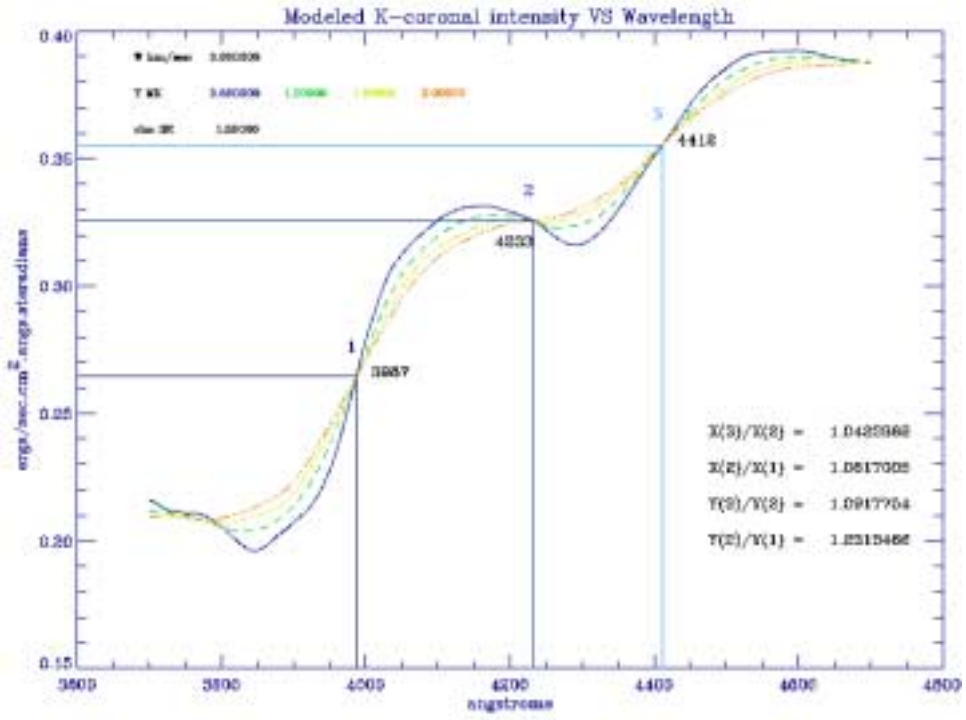

Figure (2.5). Modeled K-coronal intensity spectrum against wavelength for different isothermal coronal temperatures for a given line of sight at 1.5 solar radii.

From these modeled K-coronal intensity spectra for lines of sight at different heights off the solar limb, as depicted in figure (**2.3**), figure (**2.4**) and figure (**2.5**), Cram (1976) made two very important observations.

(a) The existence of temperature insensitive nodes in the K-coronal intensity spectra for various isothermal coronal temperatures.

(b) The remarkable independence of the positions of these nodes on the wavelength scale for lines of sight at various heights above the solar limb.

From the above two properties for the K-coronal spectrum it is now possible to implement a temperature diagnostic scheme for the measurement of the coronal temperature by means of measuring the K-coronal intensity spectrum. For this purpose suitable intensity ratios have to be determined at wavelength positions where sufficient temperature dependent parameterization of the shape could be considered. In this regard, from figure (**2.3**)-(**2.5**), it is evident that the suitable wavelength positions occur at 3850.0 angstrom and 4100.0 angstroms, respectively, which are also anti-nodes. Figure (**2.6**) is a plot of the K-coronal intensity ratios at 3850.0 angstrom to 4100.0 angstrom, from the K-coronal models for different isothermal coronal temperatures, against the temperatures.

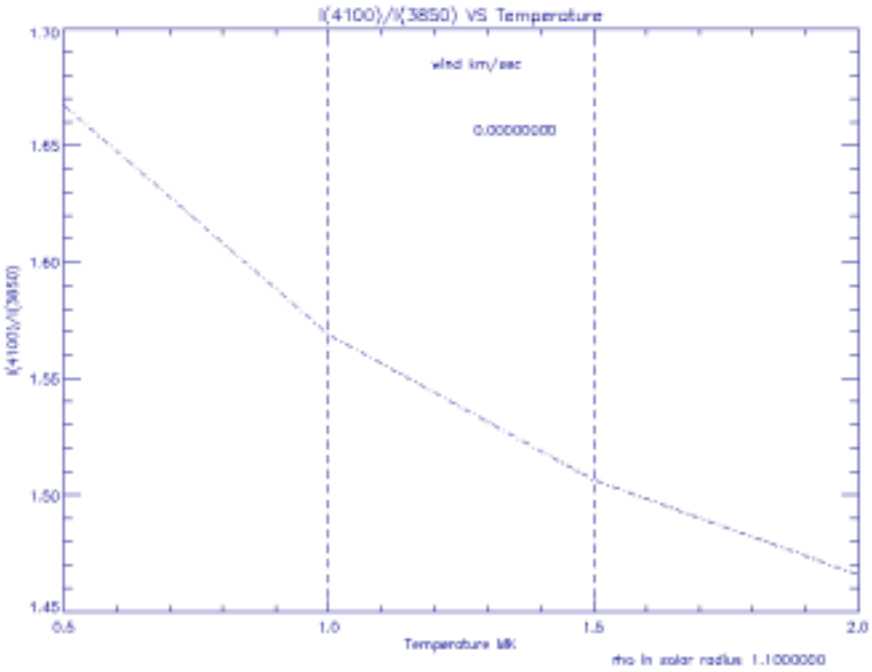

Figure (2.6). This is a plot of the K-coronal intensity ratios at 3850 .0 to 4100.0 angstroms against the assumed isothermal coronal temperatures. The ratios were calculated from the modeled K-coronal spectra for different temperatures shown in figure (2.3). These values pertain to a line of sight at 1.1 solar radii.

It is apparent from figure (**2.6**) that the coronal temperature could be determined by measuring the K-coronal intensity ratio at 4100.0 to 3850.0 angstroms from an observed K-coronal spectrum. Also from figure (**2.6**) it can be shown that if the above K-coronal intensity ratio could be determined within uncertainty of $\pm$ 1.0% then the coronal temperature could be inferred within an uncertainty of $\pm$ 0.2 MK. However it is unfortunate that the intensity measurement at 3850.0 angstrom lies in the blue end of the spectrum, which is subject to atmospheric absorption. This requires special chemical coated optics for signal enhancement. Below 3700.0 angstrom difficulties arise from the wavelength dependent atmospheric extinction while above 4700.0 angstrom the spectrum becomes relatively temperature insensitive.

The feasibility of this method for the determination of the electron temperature in the solar corona, as first suggested by Cram (1976), was demonstrated by Ichimoto et al. (1996). Ichimoto et al. (1996) used a slit spectrograph for spectroscopic observation on the solar corona during the total solar eclipse of 3 November 1994 in Putre, Chile. By isolating the K-coronal spectra form the observed total coronal spectra temperatures of 1.07 MK and 1.71 MK were determined for the base of a coronal hole and a streamer, respectively. They also reported cirrus covering of the sky during the totality, which had caused some difficulties in the analyses.

2.6 Further explanation for the formation of the temperature sensitive anti-nodes

To adequately answer the reason for the formation of the temperature sensitive anti-nodes three simple intensity profiles are considered as input intensity spectra in order to understand the scattered intensity spectra produced by the theory. Figure (**2.7**) shows an absorption line centered at 4000.0 angstrom with a FWHM (Full width at half maximum) of 40.0 angstrom on an otherwise uniform continuum. In this example the intensity spectrum shown by figure (**2.7**) is assumed to be the sun spectrum as observed from earth.

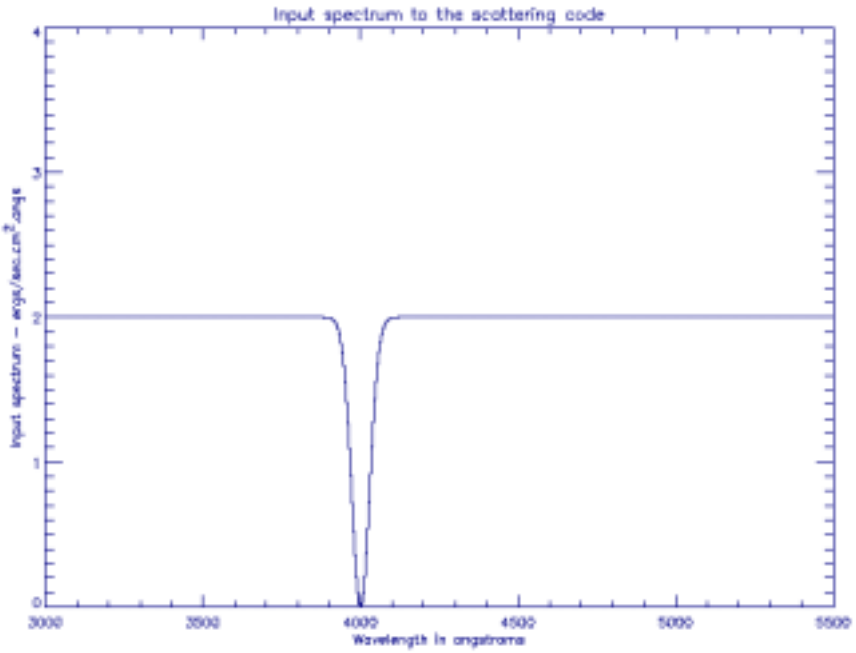

Figure (2.7). An input intensity spectrum containing an absorption line centered at 4000.0 angstrom with a FWHM of 40.0 angstrom in an otherwise uniform continuum.

Figure (**2.8**) shows the theoretical scattered K-coronal intensity spectrum for an input spectrum given by figure (**2.7**). This intensity spectrum was obtained by allowing to be scattered off the coronal electrons. The theory assumes an isothermal corona of temperatures 0.5 MK. 1.0 MK, 1.5 MK and 2.0 MK. The essential feature observed in the scattered intensity spectrum is that the smearing of photons by coronal electrons fills in the deepest absorption thus making the absorption at the line center shallower. This smearing process increases with increasing temperatures, which in essence increases the Thermal Doppler Broadening as given by equation (**2.2**). The essential point is that the intensity of radiation at line center increases as the temperature of the scattering electrons increases.

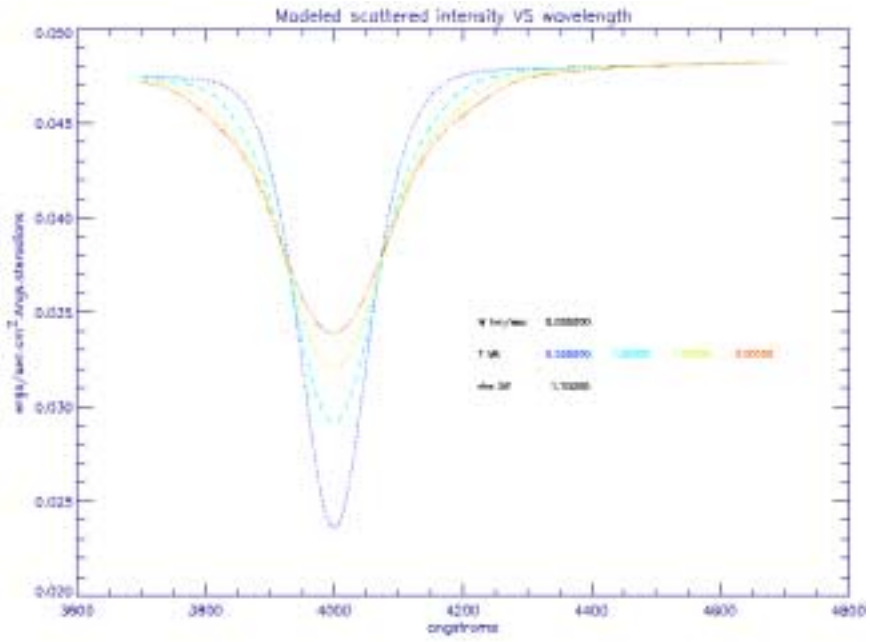

Figure (2.8). The theoretical scattered intensity spectrum by the coronal electrons for an input spectrum given by figure (2.7). The theory assumes an isothermal corona. The plots show that the smearing of the absorption line in the scattered increases with increasing temperatures.

In figure (**2.8**), the gradient d(Intensity)/d(Temperature) is positive at line center. In order to ascertain the behavior for an input intensity spectrum with two identical absorption features consider figure (**2.9**) where two strong absorption lines are centered at 400.0 and 4500.0 angstroms in an otherwise uniform continuum.

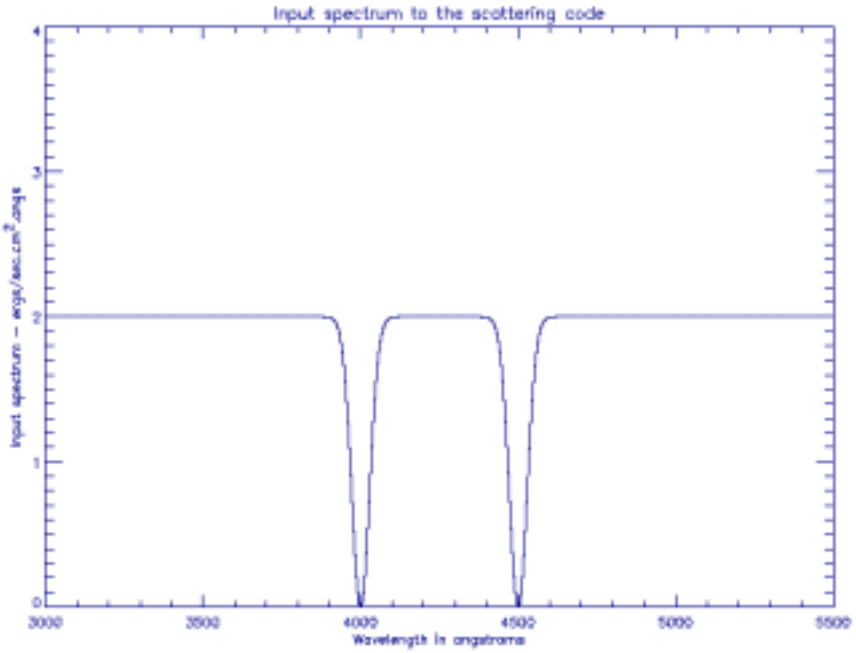

Figure (2.9). An input intensity spectrum containing two absorption lines centered at 4000.0 and 4500.0 angstroms with a FWHM of 40.0 angstrom in an otherwise uniform continuum.

Figure (**2.10**) shows the theoretical scattered K-coronal intensity spectrum for an input spectrum given by figure (**2.9**). Here we see that whereas the centers of absorption lines are filled in more and more as the temperature increases, the continuum between the line centers become progressively fainter as temperature increases. Therefore, at wavelength between the two lines (4100 – 4400 angstroms), the intensity of the continuum has a gradient d(Intensity)/d(Temperature) which is negative. This is in

striking contrast to the positive gradient d(Intensity)/d(Temperature) at line centers. It is this different behavior between line and non-line intensities that gives rise to anti-nodes, and provides the basis for Cram's method. The reason for the difference in the depths of the absorption lines is due to the effect of the temperature dependent limb-darkening coefficient.

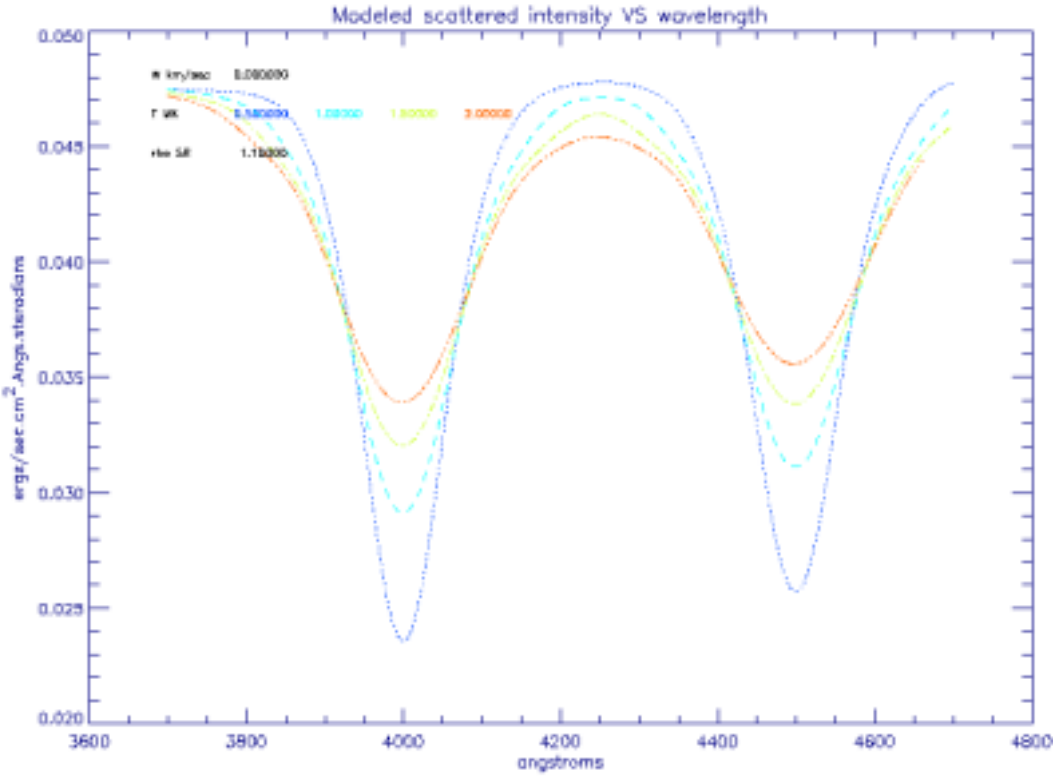

Figure (2.10). The theoretical scattered intensity spectrum by the coronal electrons for an input spectrum given by figure (2.9). The theory assumes an isothermal corona. The difference in the depths of the absorption lines in the scattered spectrum is due to the wavelength dependent limb-darkening coefficient.

Now consider the implications of introducing an emission line between the two absorption lines in an otherwise uniform continuum as shown in figure (**2.11**). Here the absorption lines are centered at 4000.0 and 4500.0 angstroms while the emission line is centered at 4250.0 angstrom with both the absorption and the emission lines with a FWHM of 40.0 angstrom. Figure (**2.12**) shows the theoretical scattered K-coronal spectrum for an input spectrum given by figure (**2.11**).

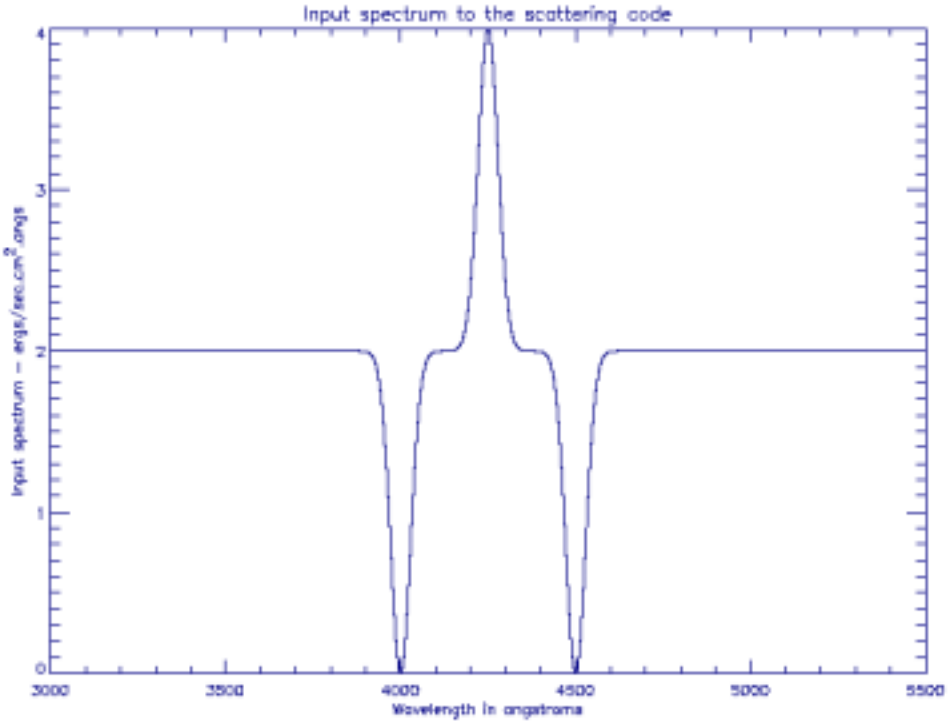

Figure (2.11). An input intensity spectrum consisting of two absorption lines centered at 4000.0 and 4500.0 angstroms while an emission line centered at 4250.0 angstrom and with a FWHM of 40.0 angstrom for the absorption and emission lines in an otherwise uniform continuum.

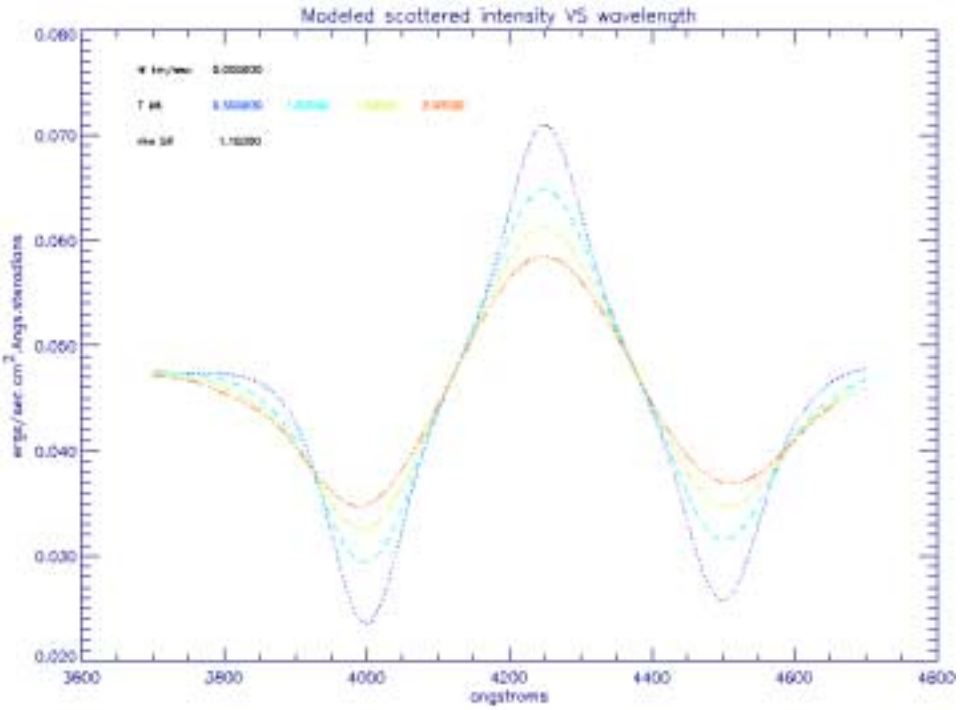

Figure (2.12). The theoretical scattered intensity spectrum by the coronal electrons for an input spectrum given by figure (2.11). The theory assumes an isothermal corona. The difference in the depths of the absorption lines in the scattered spectrum is due to the wavelength dependent limb-darkening coefficient.

With the introduction of the emission line it is evident that in the scattered K-coronal intensity spectrum, as shown in figure (**2.12**), the absorption lines become shallower while the emission line peak becomes reduced in strength. This again gives rise to the intensity on one side of the node to decrease while the intensity on the other side increase. In analogy, when the input spectra of the examples shown in figure (**2.7**), figure (**2.9**) and figure (**2.11**) are substituted by the photospheric spectrum the dips in the photospheric spectrum are progressively filled in while the higher points are progressively reduced, giving rise to anti-nodes. This is true of an integral over

wavelength of the product of the photospheric spectrum and a Gaussian kernel whose half-width lies in the range of 50 – 200 angstroms.

In the solar spectrum, the anti-nodes in the wavelength region 3900 – 4500 angstroms owe their existence mainly to two wide and strong absorption features: (1) a pair of lines labeled H and K by Fraunhofer at 3968.5 and 3933.7 angstrom, respectively; (2) the combined effects of the Fraunhofer G band at 4300 - 4320 angstroms and the Fraunhofer feature $\mathbf{H}_{\gamma}$ at 4340.5 angstrom. The G-band is a collection of closely spaced absorption lines predominantly due to the diatomic radical CH and iron.

In essence, the uniqueness of the spectral region around 4000 angstrom for the formation of the anti-nodes arises from the following coincidences. On the one hand, the H and K lines happen to provide essentially a single absorption feature with a width of tens of angstroms. On the other hand, the only molecular band that contributes significantly to the visible solar spectrum (the G-band: almost 100 detectable lines within a range of 60 angstroms) happen to lie within a few tens of angstroms of a strong atomic line $\mathbf{H}_{\gamma}$. Both of these strong absorption features are readily identifiable in the low-resolution solar spectrum shown in figure (**2.13**): the figure is taken from Cram (1976) with his theoretical K-coronal spectra superposed. Note that in low-resolution, the solar photospheric spectrum between 4000 and 4300 angstroms has corrugations that give the impression of “quasi-emission lines”. For this reason, when we were modeling the

scattering of synthetic solar spectra above, as shown in figure (**2.11**), we included an emission feature between the two absorption lines.

Are there any other parts of the solar spectrum that might be useful to test Cram's idea? It seems unlikely. If we go shortward in wavelength from 3800 angstrom, the solar flux becomes rapidly so low that it is difficult to obtain adequate signal to noise ratio. And if we go to longer wavelengths we do not find pairs of strong absorption features that are wide enough to remain detectable when we smooth them by many tens of angstroms.

The difference in the intensity of the photospheric spectra given by figure (**2.1**) and figure (**2.13**) is due to the units of measurement. In figure (**2.1**) the photospheric intensity in given in units of ergs/sec.cm^2.angstrom while in figure (**2.13**) the intensity is given in units of ergs/sec.cm^2.angstrom.steradians. To reconcile the photospheric intensities between figure (**2.13**) and figure (**2.1**) the latter needs to be divided by the solid angle of the sun's disk, which is $\mathbf{6.8\times10^{-5}}$. The differences in the intensities of the K-coronal spectra, given by figure (**2.3**) and (**2.13**), owe to the different electron number density profiles and the line of sight chosen for the analyses.

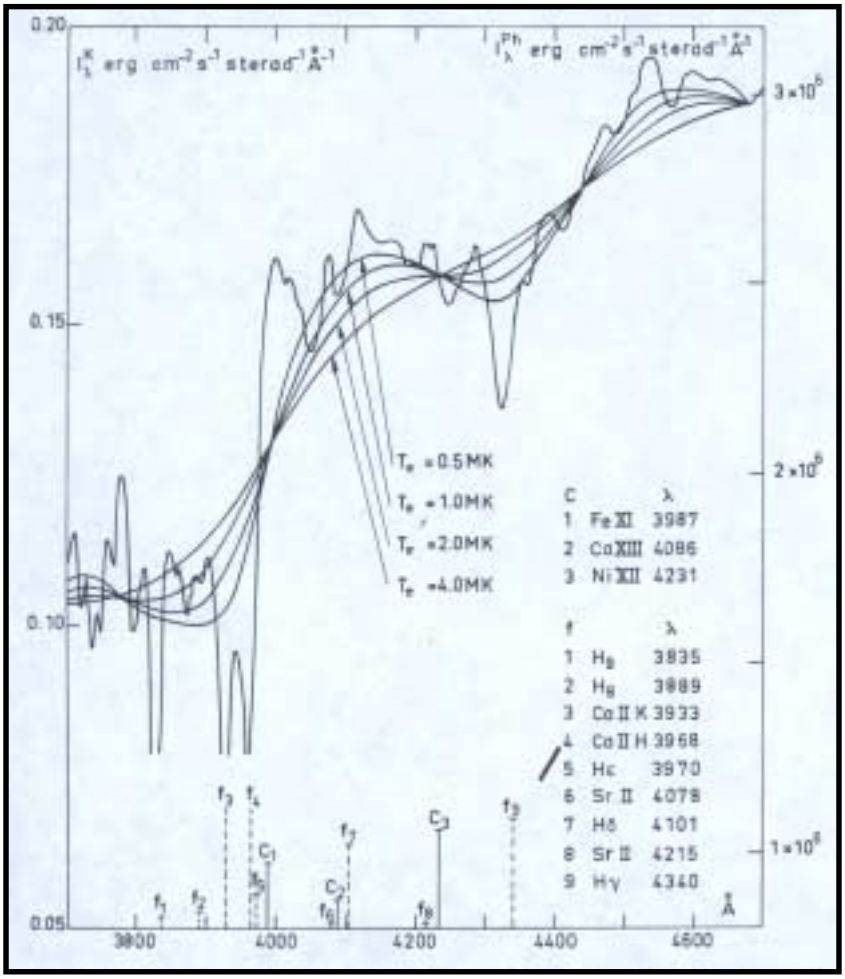

Figure (2.13). This figure shows the theoretical K-coronal intensity spectra for four isothermal coronal temperatures whose electron density is given by equation (5.8). The absolute intensity of the disk center photospheric spectrum is also shown. The vertical bars at the bottom of the figure indicate the relative strengths of the three coronal lines "c", and nine flash spectrum lines "f".

Reproduced from Cram (1976).

2.7 The influence of the solar wind on the K-coronal spectrum

The solar wind is an inherent property of the hot solar corona, a constant outflow of gas into interplanetary space. There the coronal electrons in the vicinity of the solar limb can be assumed to have a bulk outflow velocity equivalent to the solar wind velocity. In the vicinity of the sun this flow is radial and begins to take a spiral pattern at large distances, which is attributed to the rotation of the sun. However these flow velocities are latitude dependent with the fastest outflows occurring in the coronal holes.

Figure (**2.14**) is a schematic diagram to explain the redshift induced on the K-coronal spectrum by the radially outflowing coronal electrons due to the solar wind. For the illustration of the above consider three electrons located at positions 1,2 and 3 on the line of sight. All three electrons are embedded in a radially directed out flow: the magnitude of the outflow velocity is the same at three electrons, but the velocity vectors point in different directions. Electrons 1 and 3 are symmetrically located on either sides of electron 2 while electron 2 is located at the closest point on the line of sight to the center of the sun. Since they are all moving away from the sun the photospheric radiation incident on these electrons are redshifted in the frame of reference of the electrons. Furthermore, for Thomson scattering, the photospheric radiation scattered off these electrons is wavelength independent in the reference frame of the electrons and they scatter a fraction of this incident radiation along the line of sight of the observer. In figure (**2.14**), the electrons 1 and 3 have common line of sight velocity magnitudes, away and towards the observer, respectively. This allows for the scattered radiation off

electrons 1 and 3 to be red and blue shifted, respectively, in the frame of reference of the observer, thus rendering a canceling effect on the observed radiation from these two electrons. However the line of sight velocity of electron 2 is zero, which simply scatters the redshifted radiation incident on it without causing anymore wavelength shifts. Thus the Doppler shifting of the radiation scattered by these three electrons is dominated by the effect due to electron 2, which is an overall redshifting of the scattered radiation along the line of sight.

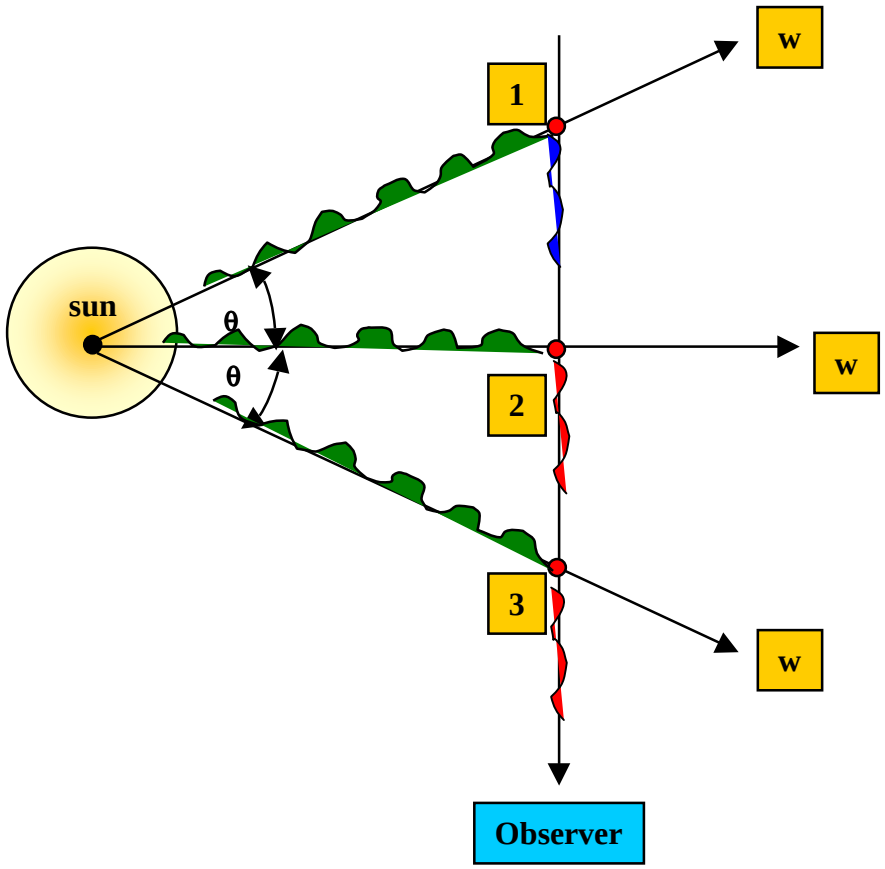

Figure (2.14). This is a schematic drawing to illustrate the redshifting of the photospheric radiation scattered off the coronal electrons, which are radially flowing away from the sun at a uniform velocity (w). Electron 2 is located at the closest point on the line of sight to the center of the sun. Electrons 1 and 3 are located symmetrically on either sides of electron 2.

The magnitude of this redshift on the K-coronal spectrum for an incident radiation of 4000.0 angstrom on the coronal electrons with an outflow velocity of 300.0 km/sec in a million degree Kelvin Corona is, from equation (**2.2**), ~4.0 angstrom. Figure (**2.15**) is a reproduction of figure (**2.1**) with horizontal bars to emphasize the magnitude of the thermal Doppler broadening and the redshift associated with the solar wind velocity. For this illustration these quantities are calculated for an incident wavelength of 4000.0 angstrom on the coronal electrons, which are radially outflowing at a velocity of 300.0 km/sec in a million degree Kelvin corona.

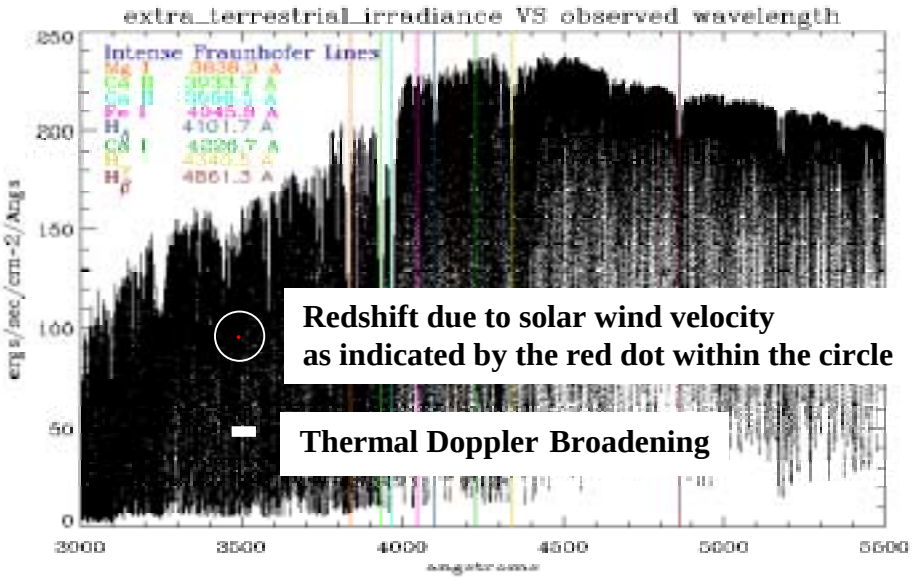

Figure (2.15). This figure shows the scale of the thermal Doppler broadening and the redshift associated with the solar wind velocity in the wavelength scale in comparison to the features of the photospheric spectrum. The scale of the redshift is shown by a red dot, which is highlighted by a circle. This comparison is made for an incident wavelength of 4000.0 angstrom on the coronal electrons, which are radially outflowing at a velocity of 300.0 km/sec in a million degree Kelvin corona.

The effect of the solar wind velocity in the model for the formation of the K-corona was considered to be negligible by Cram (1976). However an interesting additional property was revealed by the inclusion of a constant radial solar wind velocity to Cram's model. That is the temperature insensitive nodes, which were observed by Cram (1976), were now observed to shift in wavelength positions with increasing solar wind velocity while maintaining the remarkable independence of the nodal positions with height above the solar limb. Figure (**2.16**) and figure (**2.17**) are K-coronal intensity models for different isothermal coronal temperatures at a line of sight at 1.1 solar radii with assumed radial solar wind velocities of 400.0 km/sec and 800.0 km/sec, respectively.

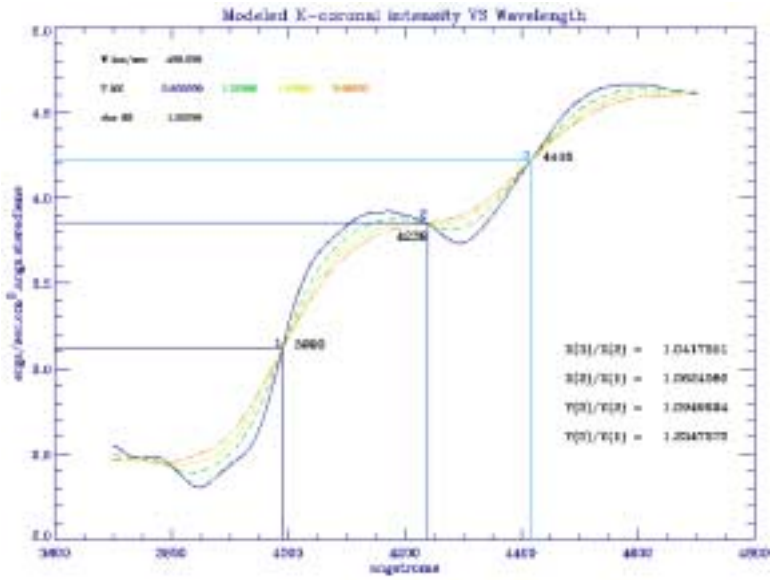

Figure (2.16). Modeled K-coronal intensity against wavelength for different isothermal coronal temperatures, for line of sight at 1.1 solar radii and a wind velocity of 400.0 km/sec.

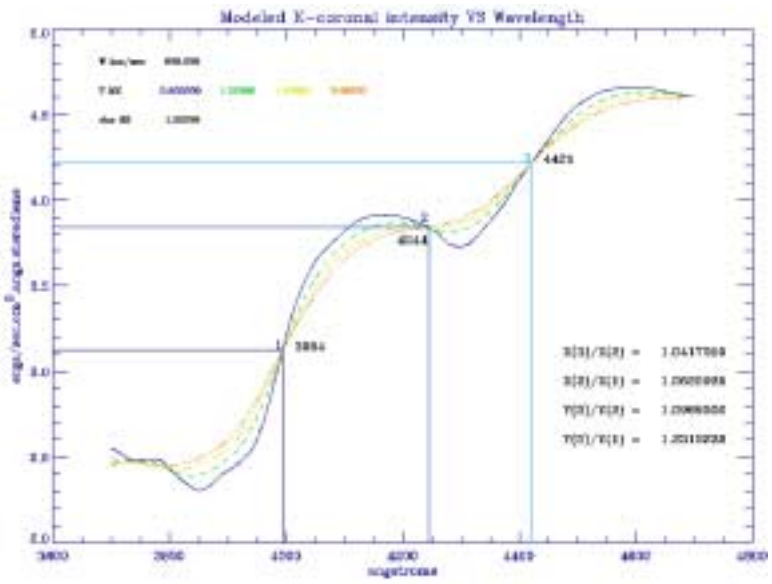

Figure (2.17). Modeled K-coronal intensity against wavelength for different isothermal coronal temperatures, for line of sight at 1.1 solar radii and a wind velocity of 800.0 km/sec.

Comparing figure (**2.16**) and figure (**2.17**) with figure (**2.3**), which is a K-coronal model for zero wind velocity, it is evident that the temperature insensitive nodes shift in wavelength positions with increasing solar wind velocities. This newfound physical property pertaining to the shifting in the wavelength positions of the temperature insensitive nodes with increasing solar wind velocities can be utilized to construct wind sensitive diagnostics.

Figure (**2.18**) is a plot of the K-coronal intensity model for different wind velocities ranging from 0.0 km/sec to 900.0 km/sec in intervals of 100.0 km/sec for an isothermal coronal temperature of 1.0 MK with the line of sight at 1.1 solar radii. It is evident from figure (**2.18**) on the existence of a wind insensitive node at 4233.0 angstrom with the maximum spread in intensity (anti-node) at 3987.0 angstrom. This property holds for other isothermal coronal temperatures and heights above the solar limb too.

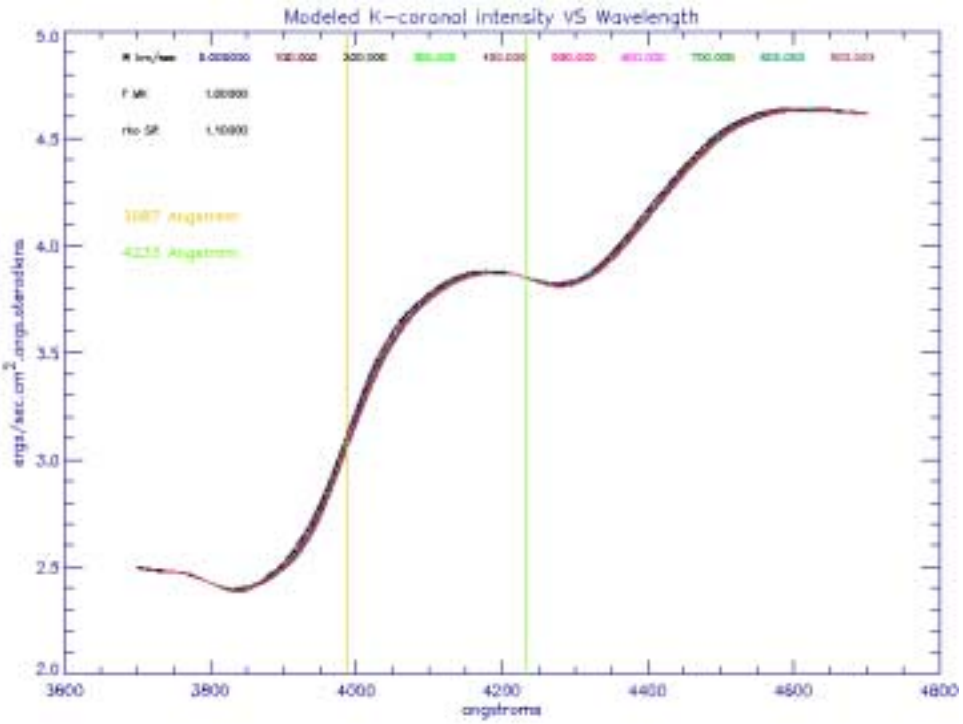

Figure (2.18). Modeled K-coronal intensity against wavelength for solar wind velocities of 0.0 km/sec to 900.0 km/sec in intervals of 100.0 km/sec, for line of sight at 1.1 solar radii and an isothermal coronal temperature of 1.0 MK.

Thus the summary of the theoretical observations on the modified version of the Cram's model, with the inclusion of the solar wind velocity is,

(a) The existence of temperature sensitive anti-nodes at certain wavelengths in the K-coronal intensity spectrum provides a meaningful temperature diagnostics.

(b) The wavelengths of the anti-nodes are remarkably independent of heights above the solar limb.

(c) The simultaneous existence of nodes in the spectrum, where temperature effects are negligible, enables us to develop a diagnostic of wind speed that is more or less independent of temperature.

2.8 Simultaneous determination of the coronal temperature and the solar wind velocity

From the theoretical properties observed from the modified Cram's model it is evident on the existence of both temperature and wind diagnostics. Figure (**2.19**) is a plot of the intensity ratios at the anti-nodes 3850.0 to 4100.0 angstroms against isothermal coronal temperatures for a range of solar wind velocities from 0.0 km/sec to 900.0 km/sec and with the line of sight at 1.1 solar radii. It too reveals the feasibility of the coronal temperature measurement within an uncertainty of $\pm$ 0.2 MK if the above intensity ratio at the anti-nodes 3850.0 to 4100.0 angstroms could be experimentally determined within

an uncertainty of ± 1.0 %. The width at the low end of the temperature range is ~0.02 MK over a wind velocity range of 0.0 km/sec to 900.0 km/sec.

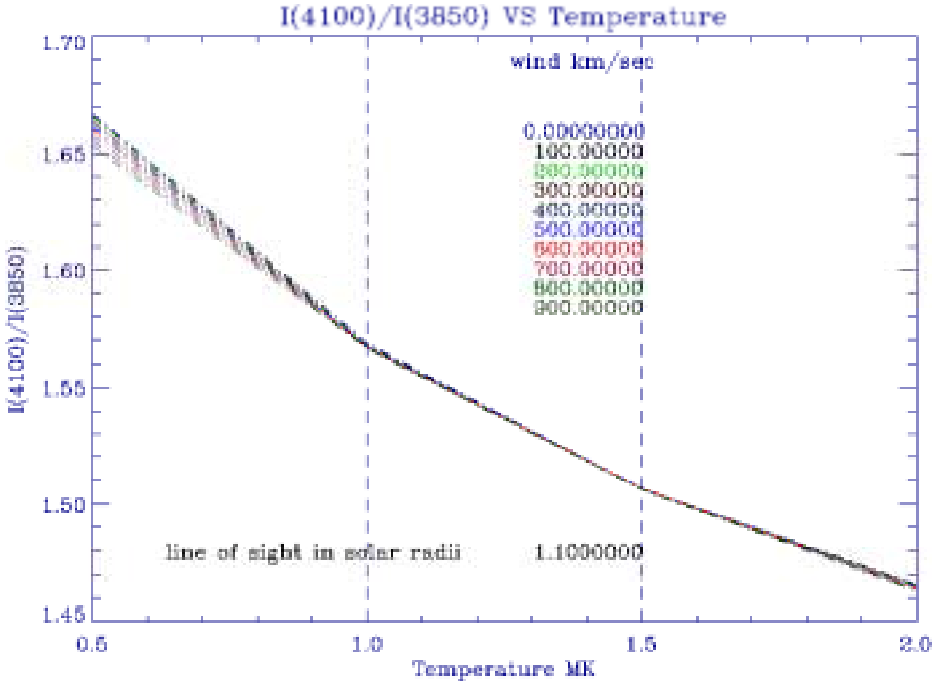

Figure (2.19). The intensity ratio at 3850.0 to 4100.0 angstroms against isothermal coronal temperatures for a range of solar wind velocities with the line of sight at 1.1 solar radii. The horizontal spread in the low end of the temperature scale is ~0.02 MK over the velocity range of 0.0 km/sec to 900.0 km/sec.

Figure (**2.20**) is a plot of the intensity ratios of the wind sensitive anti-node at 3987.0 to the wind insensitive node at 4233.0 angstroms against solar wind velocities for a range of isothermal coronal temperatures with the line of sight at 1.1 solar radii. The solar wind velocity can be determined by first determining the temperature from figure (**2.19**) and then by plotting in figure (**2.20**) the intensity ratios of the wind sensitive anti-

node at 3987.0 to the wind insensitive node at 4233.0 angstroms against the wind velocities at this temperature. Here the solar wind velocity measurements are highly sensitive to the wind-sensitive intensity ratio measurements. An uncertainty of ± 1.0 % in the wind-sensitive intensity ratio measurements can cause an uncertainty of ± 200.0 km/sec at 0.50 MK. This uncertainty increases with increasing coronal temperatures.

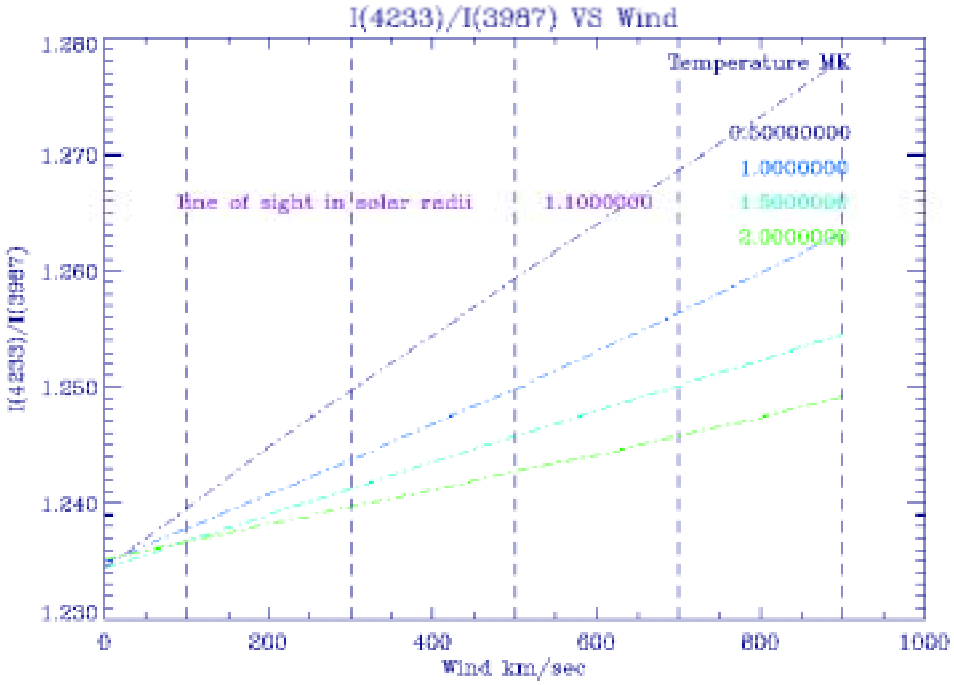

Figure (2.20). The intensity ratio at 3987.0 to 4233.0 angstroms against solar wind velocities for a range of isothermal coronal temperatures with the line of sight at 1.1 solar radii. To determine the wind velocity, first the temperature has to be determined from figure (2.19). Then the K-coronal models need to be created for a range of wind velocities at this temperature and plotted in figure (2.20).

2.9 Global determination of the coronal temperature and the solar wind velocity

In section (**2.7**) a methodology was developed to simultaneously determine both the coronal temperature and the solar wind velocity from the same wavelength dispersed K-coronal intensity spectrum. That is, by measuring the intensity ratios at 3850.0 angstrom to 4100.0 angstrom and 3987.0 angstrom to 4233.0 angstrom, from the observed K-coronal spectrum. The former is termed the, '**temperature-sensitive'** intensity ratio, which allows for the temperature measurements from figure (**2.19**). The latter is termed the, '**wind-sensitive'** intensity ratio, which allows for the wind measurements from figure (**2.20**). However for the wind measurement, further theoretical K-coronal models need to be created for various wind velocities using the measured temperature as the isothermal coronal temperature. From these models the wind-sensitive intensity ratios are plotted against the wind velocities assumed for those models in figure (**2.20**). Now by calculating the wind-sensitive intensity ratio from the observed K-coronal spectrum its corresponding wind velocity can be obtained.

In order to extend this measurement globally on the solar corona the wavelength dispersed K-coronal intensities need to be measured simultaneously and globally on the solar corona. Chapter-**3** explains an instrument designed for simultaneous and global measurement of the wavelength dispersed coronal intensity spectra from multiple locations on the solar corona. Chapter-**4** discusses the results from the very first attempt to measure both the coronal temperature and the solar wind velocity, simultaneously and

globally, on the solar corona. This experiment was performed during the total solar eclipse of 11 August 1999 in Elazig, Turkey.

2.10 The essence of this dissertation

In this dissertation the influence of the solar wind velocity was added to the Cram's model to search for both coronal temperature and solar wind velocity diagnostics. Based on the feasibility for the measurement of the **coronal temperature** and **solar wind velocity** diagnostics, form a single spectroscopic observation of the solar corona, an instrument was designed that would **globally** and **simultaneously** measures both these quantities at twenty different locations on the solar corona (Reginald & Davila, Paper I, 2000). The very first experimental effort was carried out in conjunction with the total solar eclipse of 11 August 1999 in Elazig, Turkey and the results were analyzed to obtain both the coronal temperatures and the solar wind velocities at multiple locations (Reginald & Davila, Paper II, 2000).